24th COBEM - 2017

24th ABCM International Congress of Mechanical Engineering
December 3-8, 2017, Curitiba, PR, Brazil

COBEM-2017-0990
FLOW ANALYSIS INSIDE THE COMBUSTION CHAMBER AND THE NOZZLE OF A HYBRID ROCKET MOTOR

Paulo Gabriel Cunha Martins
Olexiy Shynkarenko
Universidade de Brasília, Faculdade UnB Gama, DF, Brazil
Universidade de Brasília, Faculdade UnB Gama, Laboratório de Aplicação e Inovação em Ciências Aeroespaciais (LAICA), DF, Brazil
paulomartins92@gmail.com
olexiy@aerospace.unb.br

Abstract. *The main objective of this work is the numerical validation of the hybrid rocket prototype developed by UnB Chemical Propulsion Laboratory (CPL) team. This rocket motor can be used in the SARA Orbital project during the induction of an atmospheric reentry maneuver in a low orbit. For this, some theoretical and numerical methods were developed to perform mass and energy flow analysis in the combustion chamber and nozzle. The initially used theoretical method was the fuel regression empirical model to calculate the behavior of the fuel port diameter throughout the firing time. With the results of this theoretical method, the numerical analysis of the behavior of the fluid including the combustion process in different time intervals was done. The numerical analysis aims to show a complete development of the compressible non-viscous and viscous flows with the combustion of nitrous oxide/paraffin propellants pair. The simulation results obtained by using ANSYS Fluent® showed good correspondence with the analytical approach. At the current paper, the numerical simulation results were analyzed and discussed, for the better understanding of the behavior of the processes in the combustion chamber, and future validation of the modeling by the CPL experimental data.*

Keywords: *hybrid rocket motor, solid fuel regression, flow simulation, rocket nozzle, combustion chamber.*

1. INTRODUCTION

This work aims to simulate numerically the operation of the SARA hybrid rocket motor designed, built and tested by the CPL UnB [Shynkarenko *et al.* (2015a) and Shynkarenko *et al.* (2015b)] considering the motor operation process in different firing stages. This rocket motor was designed to meet the conditions required to induce atmospheric re-entry of the SARA Orbital platform, so it must meet the requirements of thrust, specific impulse, mass flow, among others, in order to have a variation of orbit velocity generating induction of the re-entry maneuver into the atmosphere, [Curtis (2005)], [George P. Sutton (2010)].

In order to validate this project, the CFD analysis was carried out for the internal volume of the combustion chamber and the nozzle. The numerical simulation was necessary due to the complexity of geometry and difficulty to obtain the physicochemical properties of the propellant experimentally or analytically. The flow behavior inside the combustion chamber and in the nozzle was obtained through numerical simulation using the software ANSYS Fluent® and it was explained on the "Computational procedures" section.

This SARA hybrid rocket motor was tested safely several times from 12 to 41 seconds of burning on a horizontal test bench realized by the CPL. The numerical simulation performed on ANSYS software was stationary, with that, for a better analysis of the flow behavior during the propulsion process, there were realized three distinct stationary simulations of the combustion process on three different time moments. The simplified new geometry of the fuel grain for each instant considered were calculated through the empirical fuel regression method presented on the paper Zilliac and Karabeyoglu (2006).

In the section "Analytical procedures" were explained the steps to calculate the state of the paraffin fuel over time and the the method of the flow properties calculations for the non-viscous flow inside a nozzle, that were explained to introduce the reader the simplest case to get the flow properties distributions inside a nozzle.

The results of the numerical simulations are way more difficult to calculate analytically or even impracticable experimentally. Among the results presented on this paper are the comparison of the area facet average of pressure, temperature and velocity along the nozzle for each case considered, the combustion process for three different time moments, the simulation considering only viscous ideal gas and some data from RPA (Rocket Propulsion Analysis) software. Beyond those results there are the flow pattern and the combustion products distribution (Water and Carbon dioxide) inside the combustion chamber over different time intervals.

2. COMPUTATIONAL PROCEDURES

The numerical simulation was performed on a two-dimensional, axisymmetric surface and considering the corresponding nitrous oxide flow rates and the paraffin regression rate. The two-dimensional geometry of the combustion chamber and nozzle is shown on Figure 1.

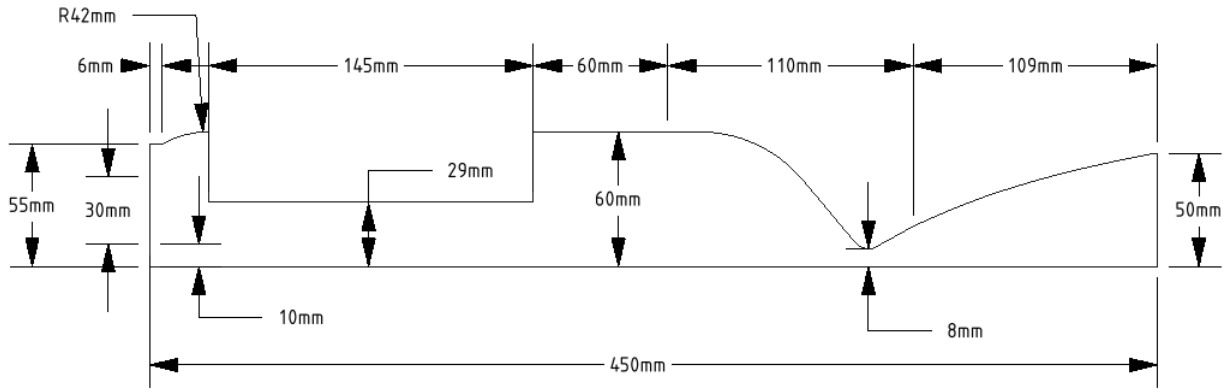

Figure 1. Complete geometry for the simulation.

The boundary surfaces with respect to the boundary conditions are indicated in the Figure 2, where in color blue are the injectors with constant mass flow rate of N2-O2 mixture and paraffin. In black color is the solid wall (with zero flux), in red color is the nozzle exit with zero pressure gradient and in green is the axis of symmetry for rotation of the surfaces described.

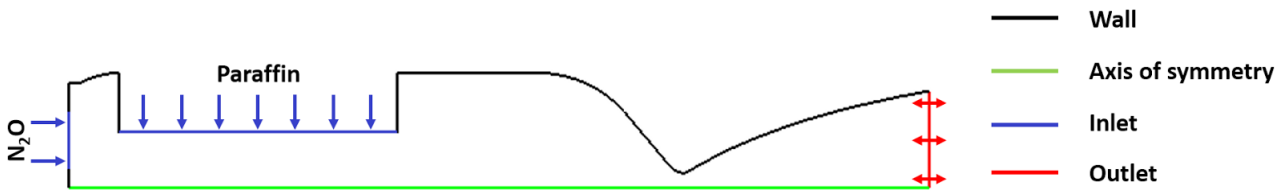

Figure 2. Boundary faces of the combustion chamber and nozzle.

The parameters of mass and mass fluxes considered on the inlet were taken from Shynkarenko *et al.* (2015b) and are listed on table 1. This simulation was designed to visualize the quantities of the properties (Pressure, Temperature, Velocity) and the distribution of the species inside the combustion chamber and nozzle when this hybrid motor is working in space.

Table 1. Parameters of mass and mass flux of the SARA motor of nitrous oxide and paraffin, Shynkarenko *et al.* (2015b)

Parameters	Mass [Kg]			Mass Flux [Kg/s]		
Components	C_nH_{2n}	N_2O	Total	C_nH_{2n}	N_2O	Total
Values	0,700	4,540	5,240	0,058	0,380	0,437

The stationary Navier-Stokes equations were supported by the Standard $\kappa-\varepsilon$ model and the Gri-Mech 3.0 combustion model available on Smith *et al.* (1999). The system was solved using pressure-based simple scheme with under-relaxation coefficients. The spatial discretization were considered standard for pressure, first order upwind for density, momentum, turbulent kinetic energy, turbulent dissipation rate and second order upwind were applied for energy, mean mixture fraction and mixture fraction variance. The boundary conditions of the simulation were the following:

- At the inlet, the mass fluxes of propellants were set according to the Table 1. In order to avoid multiphase simulation and simplify the solution, the injection of the nitrous oxide was assumed to be in the gaseous form. Since the used Gri-Mech model does not describe appropriately decomposition of the nitrous oxide and the characteristic decomposition time is short (in order of 10^{-9}s), the injected oxidizer is supposed to be decomposed close to injector and the nitrogen-oxygen mixture is therefore satisfying an approximation with this balance when it enters the

system (63,6% N2 + 36,3% O2 by mass). By the same reason, the paraffin C_nH_{2n} was assumed to be decomposed to ethylene C2H4. The thermodynamic properties of the inlet gases were re-calculated by the thermodynamic relations.

- At the outlet, the zero pressure gradient was set;
- At the axis of symmetry were set the axisymmetric conditions (velocity reflection);
- On the solid wall the adiabatic non-slipping conditions were set.

The mesh for this simulation is shown on Figure 3 and consists of 163146 elements, its distribution has a higher density near the walls in order to satisfy the $\kappa - \varepsilon$ turbulence model that require y^+ between 30 and 60. For this simulation were obtained a value of y^+=32. The model FLUID81 implemented in ANSYS Fluent® was used to generate this mesh. This model is considered to be appropriate for the axisymmetric simulations of fluids inside pipes, where the variation of pressure and temperature influence on the structure of the turbulences and the interaction between wall and fluid, ANSYS (2017).

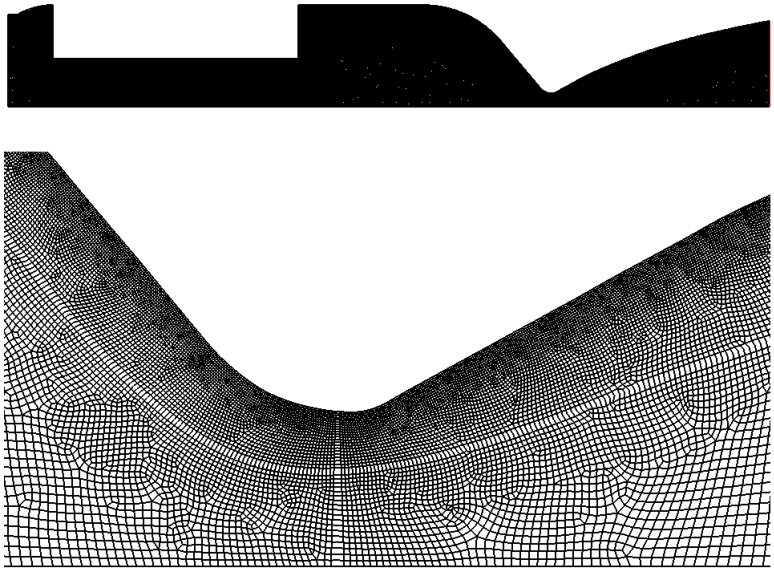

Figure 3. Distribution of the elements in the mesh over all the control volume and near the wall.

The mesh presented on figure 3 were configured with the tool "element size", that ask just for the edge of the control surface and measurement of the mesh cells in length units. The measurements and the edges selected are present on the figure 4

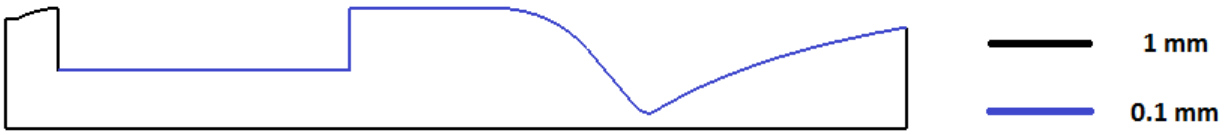

Figure 4. Element size of the mesh applied during its configuration.

3. ANALYTICAL PROCEDURES

In order to be able to obtain the flow properties during the combustion process at different time moments, the behavior of the paraffin grain was calculated numerically in MATLAB by the method of the regression of the fuel presented on the paper Zilliac and Karabeyoglu (2006).

This method is based on the resolution of the equations (1), (2) and (3) through the Runge-Kutta method, where the letter "G" is the flux of oxidant per unit of the port area, "x" is the coordinate along the length of the paraffin grain and "a", "n" and "m" are constant dependent of the grain material, the oxidant and the cross section of the paraffin grain.

$$\dot{r} = aG_{ox}^{n}x^{m} \tag{1}$$

$$G = \frac{\dot{m}}{\pi r^2} \tag{2}$$

$$r = \int_0^{tf} \dot{r}dt = r_0 + \dot{r}\delta t \tag{3}$$

Considering that (r_0, r_{12s}, $\dot{m}$) and the variation of the radius will remain constant along the longitudinal axis for simplification (m = 0), it was possible to solve the equation (3) by the Runge-Kutta method available in Matlab. With this analysis, the regression of the fuel port over time was obtained during the combustion process, as it is presented on figure 5, then it were calculated the radius of the port for different time moments presented in the table below.

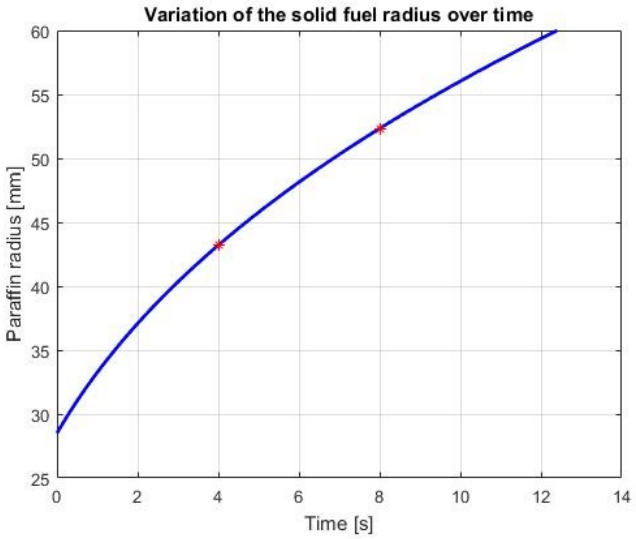

t [s]	r [mm]
0	28,50
4	43,2
8	52,33

Figure 5. Distribution of the paraffin radius over time

In order to obtain the distribution of the properties over a nozzle, such as pressure, velocity and temperature, it was considered the equations for non-viscous compressible flow presented in the Anderson Jr book [8]. Below are presented the equation (4) that relates the cross sectional area of the nozzle with the Mach number of the flow. Where $A^{\star}$ is the cross sectional area of the throat and γ is the adiabatic constant of the flow determined by RPA software and then averaged by temperature to value γ = 1.27.

$$\left(\frac{A}{A^{\star}}\right)^2 = \frac{1}{M^2}\left[\frac{2}{\gamma+1}\left(1+\frac{\gamma-1}{2}M^2\right)\right]^{\frac{(\gamma+1)}{(\gamma-1)}} \tag{4}$$

According to this function, the Mach number of the flow is related to the cross section area ratio in the nozzle, as it is presented on the equation (4) and by other hand, the properties of the flow, such as pressure, density and temperature are related to the Mach number and the adiabatic index, like it is showed in the equations for the isentropic flow (5),(6) and (7).

$$\frac{P_0}{P} = \left(1 + \frac{\gamma - 1}{2} M^2\right)^{\frac{\gamma}{(\gamma-1)}} \tag{5}$$

$$\frac{\rho_0}{\rho} = \left(1 + \frac{\gamma - 1}{2} M^2\right)^{\frac{1}{(\gamma-1)}} \tag{6}$$

$$\frac{T_0}{T} = 1 + \frac{\gamma - 1}{2} M^2 \tag{7}$$

Once those are calculated, the other properties such as sound speed and velocity can be calculated, as it is presented on the following equations (8) and (9).

$$a = \sqrt{\gamma R T} \tag{8}$$

$$V = M \times a \tag{9}$$

Presented isentropic model was used to determine the preliminary parameters of the flow inside the divergent-convergent nozzle of the hybrid motor. These data allowed to make a preliminary design of the nozzle. The profiling of the nozzle was done by the method of characteristics presented in Anderson Jr (2011).

4. RESULTS

After all the preliminary analytical procedures were done, the simulations for the times t = 0s , 4s and 8s succeeding the ignition were determined following the convergence of the residuals, presented on the figure 6. It was considered that, when the residuals of the kinetic energy of the turbulence κ and the dissipation of the turbulence ε are below the limits of 10^{-6} and the corresponding values of continuity, energy, fvar, fmean, x and y velocities were stabilized, the solution had converged and the results were determined. Due to the second order of approximation of the momentum equations, the residuals of the velocity components remained relatively high, which could be solved by adjusting the under-relaxation factors.

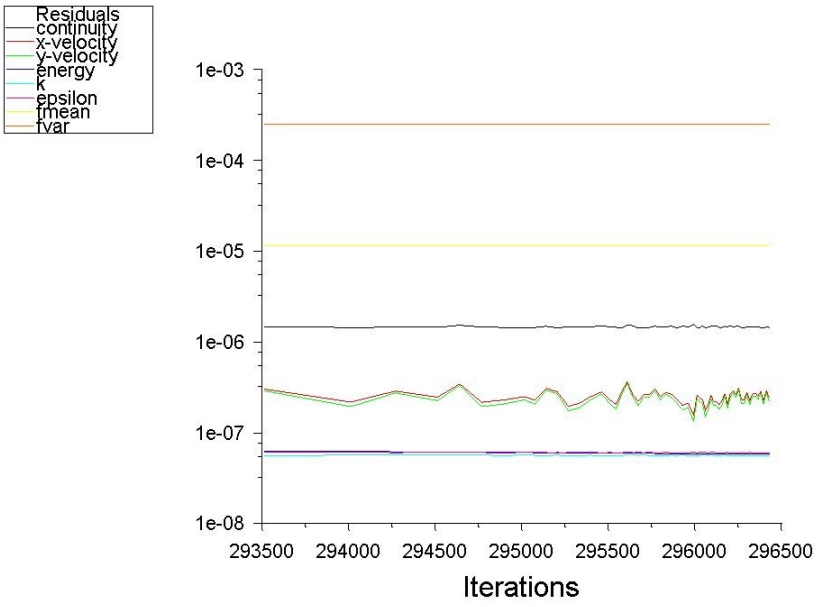

Figure 6. Simulation residuals.

The numerical simulation allowed to determine the distributions of the flow properties and the species over all the combustion chamber and nozzle. The area-averaged parameters were calculated along the convergent and divergent part of the nozzle. The facet average of the flow properties for the combustion simulations on the 3 time moments were compared with the results obtained on a simulation considering only ideal gas with viscous flow and with the results of pressure and temperature values from the RPA calculation. In the figure 7 is presented the facet average of the properties (Pressure, Temperature and Mach number) over the nozzle.

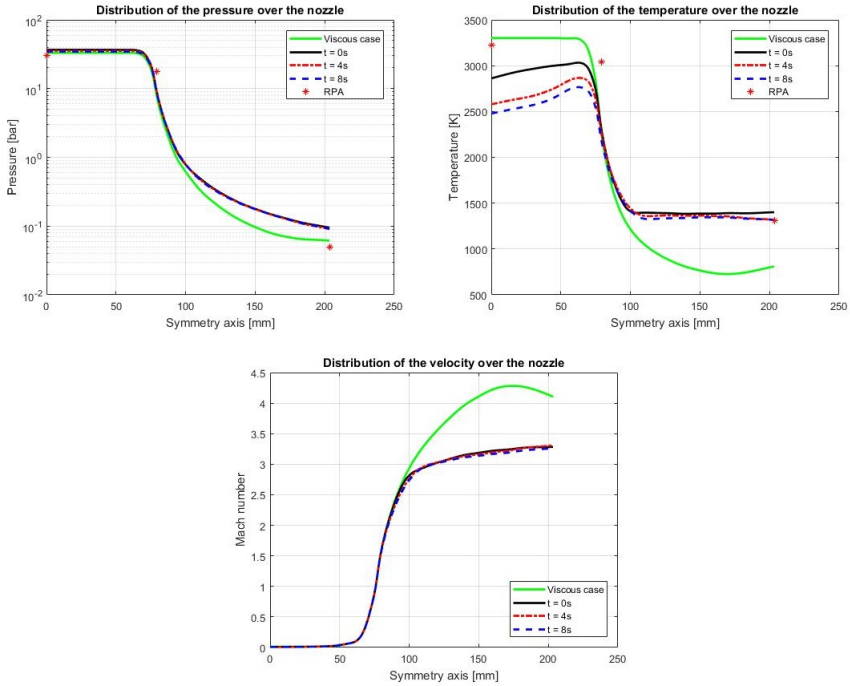

Figure 7. Distribution of Pressure, Temperature and Mach number

By comparing of simulations for the three time moments shown on figure 7, it is noted a similarity of the pressure for the combustion model, the Rocket Propulsion Analysis (RPA) and the Viscous case analyzed without combustion model (cold gas simulation).

Still it is expected a decrement of the pressure and temperature on the combustion chamber due to the growth of the combustion port during the propulsion process. For the divergent part of the nozzle it is noted that all the thermodynamic properties decrease over time, according to the theory of compressible flow, Anderson Jr (2011).

The variations of the flow in the pre-combustion chamber and post-combustion chamber were obtained for the instants of t = 0s, t = 4s and t = 8s. The path-lines of the flow are presented in the figure 8 for each instant considered.

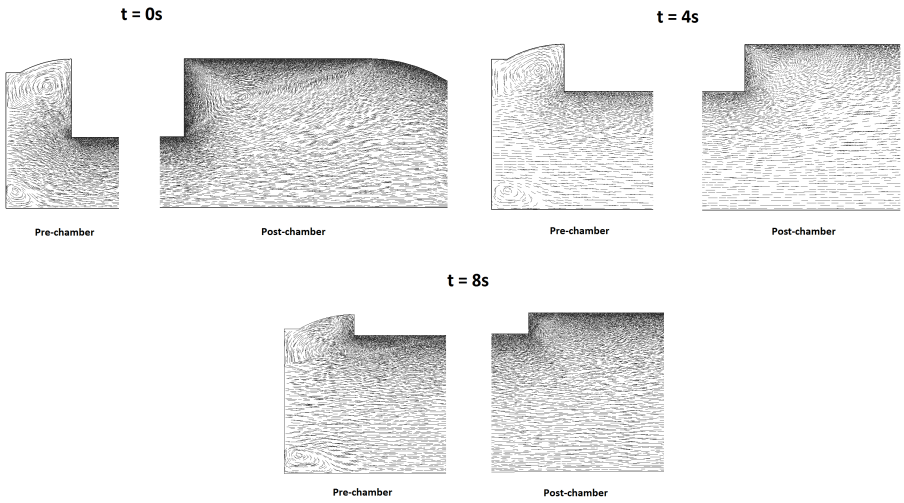

Figure 8. Pathlines of the flow in pre- and post-combustion chambers of the motor

During the propulsion process the grain keeps regressing due to its own vaporization and the vortex formation diminishes due to the geometric factors, turning the flow inside the combustion chamber smother over the time. The consequence of the vortex formation after the grain results in the transformation of the kinetic energy into thermal and potential energy and thus increases the heat transfer to the convergent part of the nozzle, with that it may be expected an increase of the temperature in this zone and a higher ablative process of the heat insulation material, Anderson Jr (2011). In the following figure 9 and 10 are presented the distributions of the products of combustion, water and carbon dioxide.

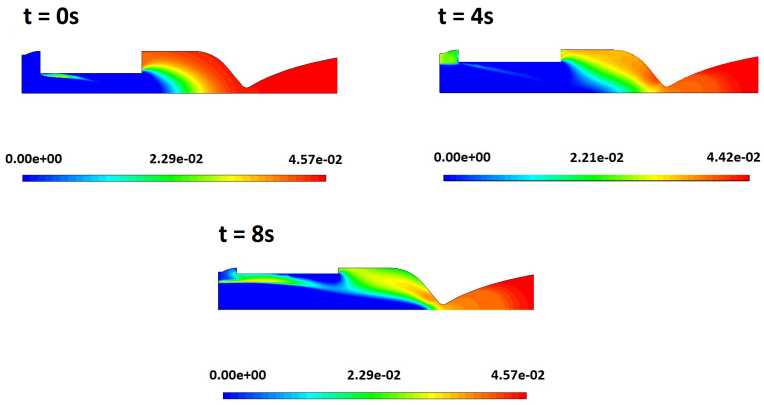

Figure 9. Concentrations of CO2.

The products of combustion, such as water and carbon dioxide, initially have the largest distribution at the convergent part and the exit of the nozzle, because the species reactions happen within the stoichiometric balance at this part. Over time these concentrations decrease, which in practice is explained by the reduction of the mass of the fuel, which is burned over time and has a "shelf life" of only 12.3 seconds.

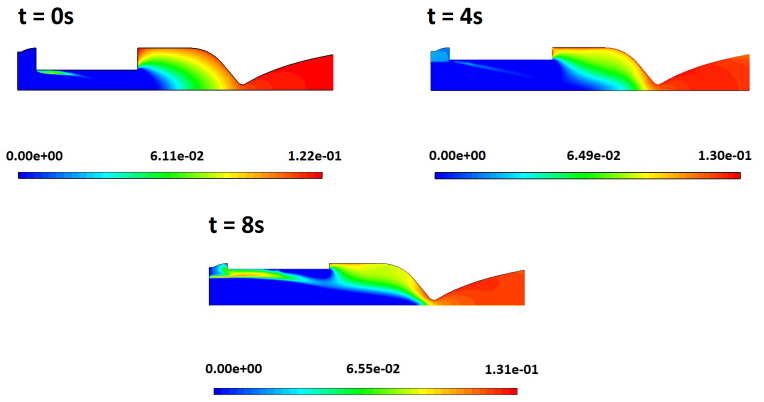

Figure 10. Concentrations of H2O.

5. CONCLUSIONS

This study made possible to establish the numerical simulation algorithm, calculate the flow properties inside the hybrid rocket motor at several time instants, and verify the distribution of the flow for an optimized combustion chamber and the nozzle geometry.

It was possible to compare the results along different time intervals during the propulsion and to check that no shock waves happen inside the nozzle, so it is expected the flow outside the nozzle working as under expanded or optimum nozzle and for consequence the nozzle won't suffer a several damage due to the ablative process in any position.

The current work does not pretend to be accurate at the processes of the fuel solid-liquid-gas transformation which happens in the combustion chamber along the grain burning. It also described the nitrous oxide behavior in a quite simplified form. However, since the conservation laws were used for the properties recalculation, we believe that the general energy balance in the system was calculated precisely. The main result of the current research was a numerical solution of the flow process with combustion in the divergent-convergent nozzle, which is quite close to the real flow process, as will be shown in the continuation of this work.

6. ACKNOWLEDGEMENTS

Authors of this work a thankful to the Brazilian Space Agency for the financial support of the current research project.

7. REFERENCES

Anderson Jr, J.D., 2011. *Fundamentals of aerodynamics*. Tata McGraw-Hill Education, 5th edition.

ANSYS, 2017. "Ansys online manuals". `http://www.ansys.stuba.sk/html/elem_55/chapter4/`. [Online; accessed 16-Juni-2017].

Curtis, H., 2005. *Orbital Mechanics for Engineering students*. Elsevier Aerospace Engineering Series.

George P. Sutton, O.B., 2010. *Rocket Propulsion Elements*. Wiley.

Shynkarenko, O., Andrianov, A. and Bertoldi, A., 2015a. "Low-thrust hybrid motor efficiency research for design optimization purposes".

Shynkarenko, O., Andrianov, A., Bertoldi, A. and Jr., M.N.D.B., 2015b. "Concept and design of the hybrid test-motor for the development of a propulsive decelerator of sara reentry capsule".

Smith, G.P., Golden, D.M., Frenklach, M., Moriarty, N.W., Eiteneer, B., Goldenberg, M., Bowman, C.T., Hanson, R.K., Song, S., Gardiner, W.C., Lissianski, V.V. and Qin, Z., 1999. "Gri mech 3.0". `http://combustion.berkeley.edu/gri-mech/index.html`. [Online; accessed 01-July-2016].

Zilliac, G. and Karabeyoglu, M.A., 2006. "Hybrid rocket fuel regression rate data and modeling". *AIAA Paper*, Vol. 4504.

8. RESPONSIBILITY NOTICE

The authors are the only responsible for the printed material included in this paper.